## Supplementary information

### i. DSC traces

DSC was applied in three cycles at 20°C/ min for the synthesized PILs.

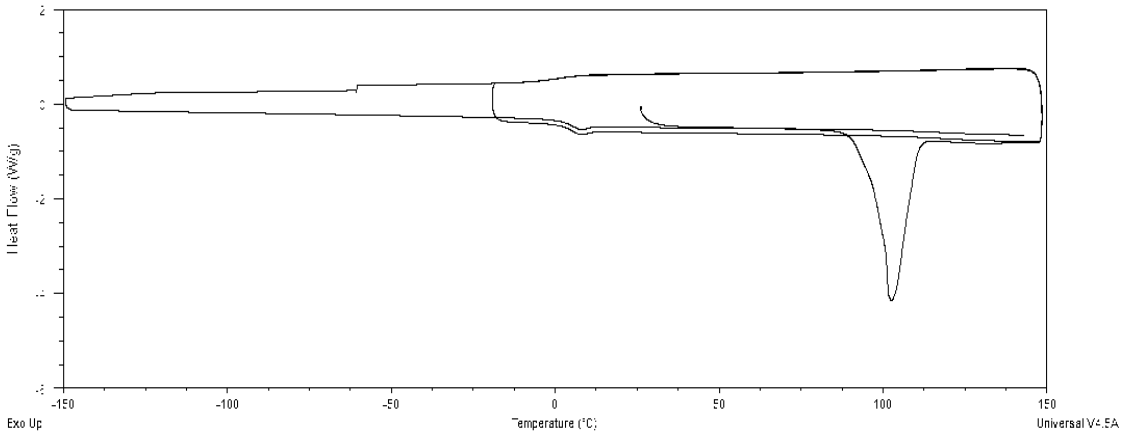


**Figure S1.** DSC trace of [ImPr][Phth]

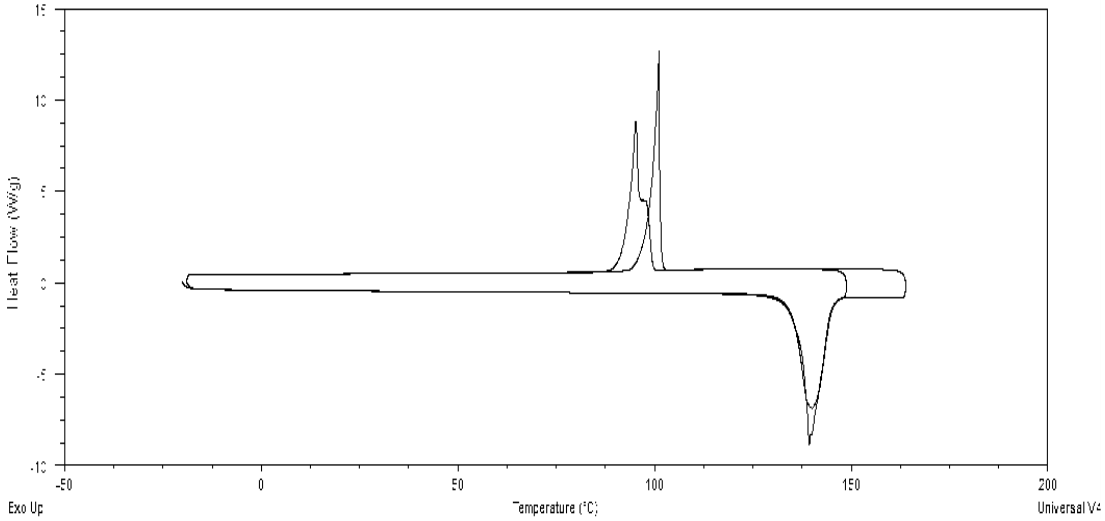


**Figure S2.** DSC trace of [ImPr][Ox]

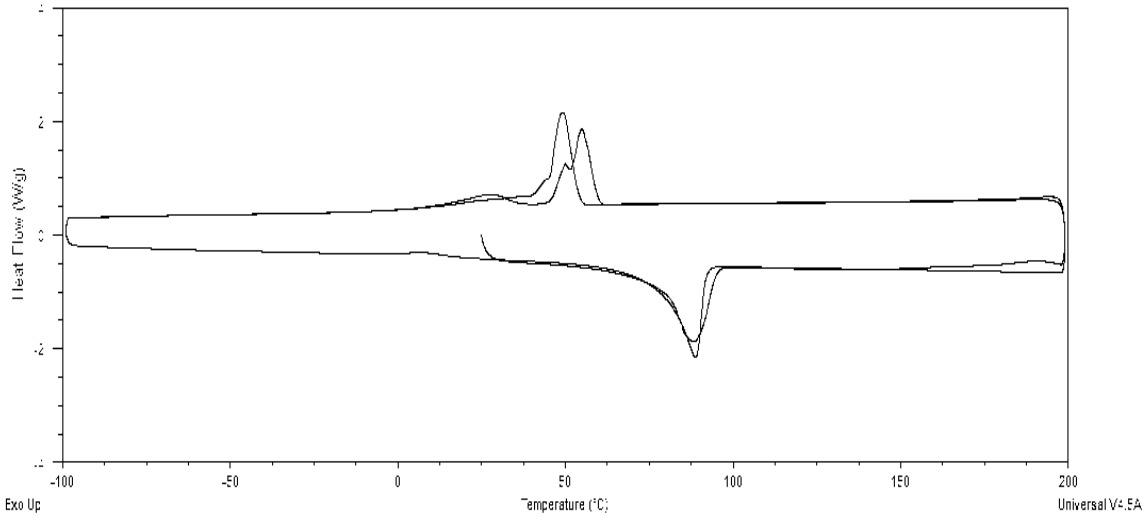


**Figure S3.** DSC trace of [ImPr][$HSO_4$]

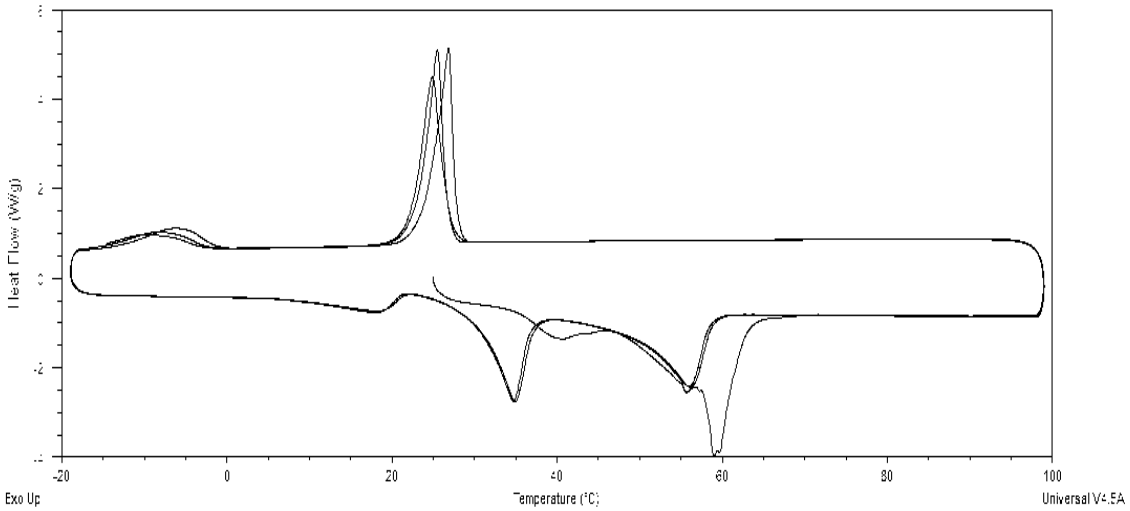


**Figure S4.** DSC trace of [ImPr][BDT]

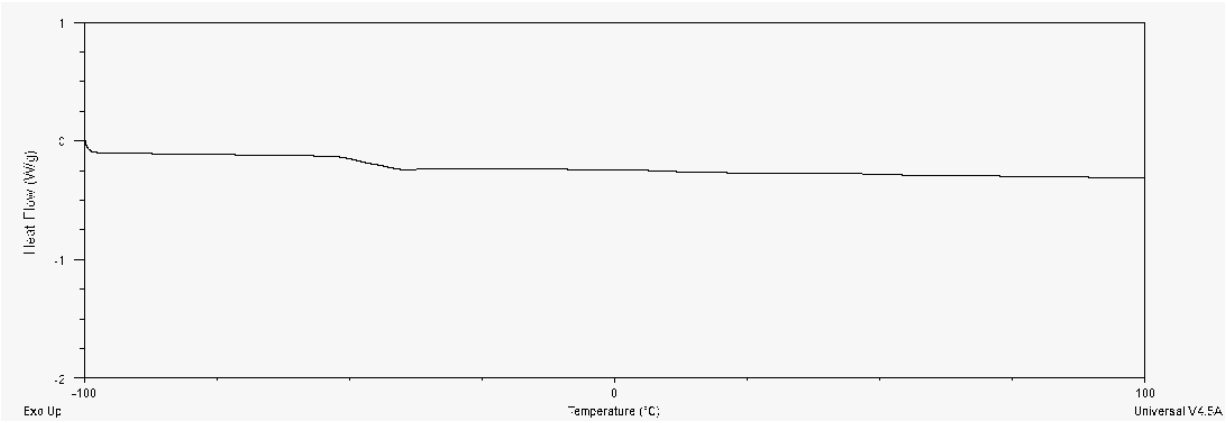


**Figure S5** DSC trace of [ImPr][Pim]

**ii. TGA and DSC**

DSC initially had been done in the range of -150 – 400ºC in one cycle at 20ºC/min. and the results have been compared with TGA data.

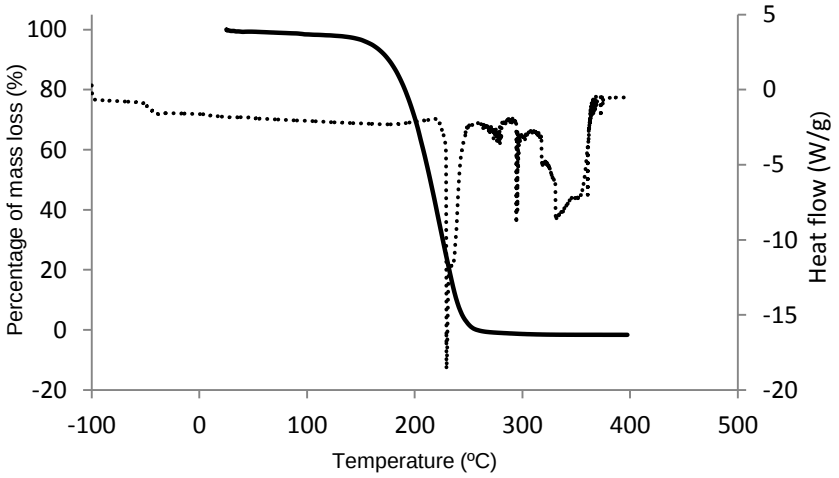


**Figure S6.** [ImPr][Pim] TGA and DSC traces

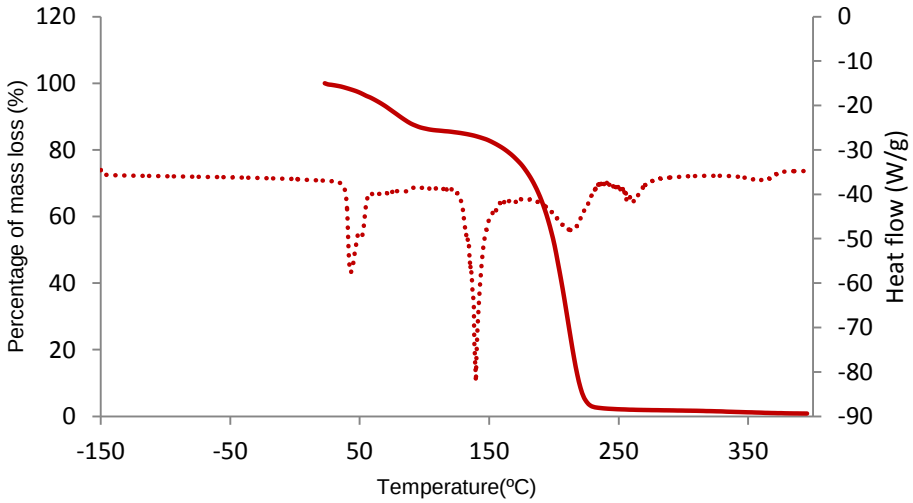


**Figure S7.** [ImPr][Ox] TGA and DSC traces

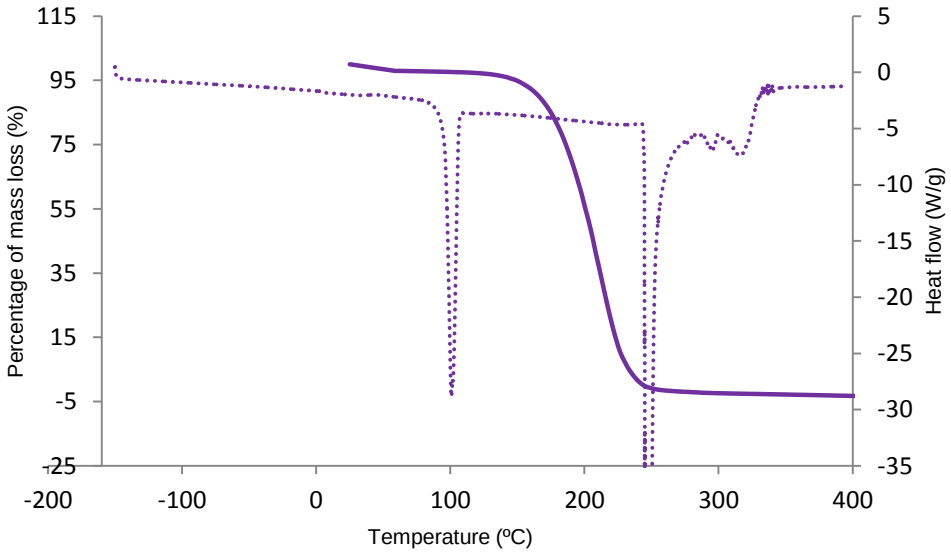


**Figure S8.** [ImPr][Phth] TGA and DSC traces

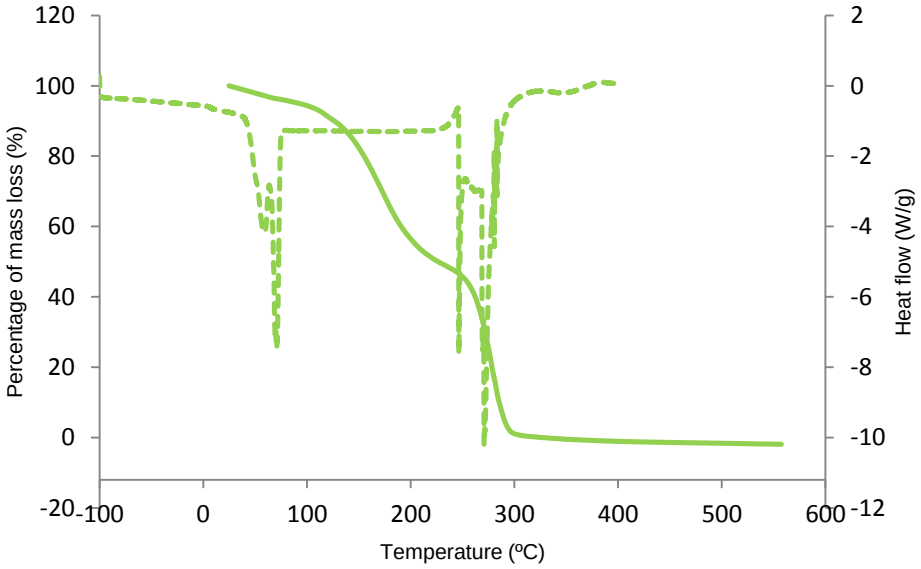


**Figure S9.** [ImPr][BDT] TGA and DSC traces

### iii. Viscosity measurement at different temperatures

**Table S1** Change in viscosity of [ImPr][Phth] as function of temperature

| Temperature(ºC) | Viscosity (Pa.s) |
|---|---|
| 31 | 236.2 |
| 32 | 213.5 |
| 33 | 185.9 |
| 34 | 168.2 |
| 35.5 | 136.2 |
| 36 | 129.7 |
| 37.5 | 109.2 |
| 38 | 97.2 |
| 39 | 91.1 |
| 40 | 79.8 |
| 42 | 62.9 |
| 43 | 55.9 |
| 44 | 48 |

| | |
|---|---|
| 46 | 39.9 |
| 47 | 35.1 |
| 48 | 31.7 |
| 49.5 | 26.7 |
| 51 | 24.7 |
| 52 | 22.6 |
| 54 | 19.9 |
| 55 | 16.4 |
| 56 | 15.8 |
| 61 | 9.9 |
| 66 | 4.8 |
| 71 | 2.3 |
| 78 | 1.5 |
| 81 | 0.9 |
| 87 | 0.4 |
| 96 | 0.3 |
| 101 | 0.2 |
| 104 | 0.2 |

**Table S2** Change in viscosity of [ImPr][Pim] as function of temperature

| **Temperature(°C)** | 15 | 20 | 25 | 30 | 35 | 40 | 45 | 50 |
|---|---|---|---|---|---|---|---|---|
| **Viscosity (Pa.s)** | 16 | 11.4 | 4 | 4.5 | 2.1 | 1.6 | 1 | 0.6 |

## IV. Ion conductivity measurement

**Table 3** Conductivity data for [ImPr][Pim] by temperature

| **1000/T ($K^{-1}$)** | **conductivity (μS/cm)** |
|---|---|
| 3.47 | 29 |
| 3.41 | 39.6 |
| 3.35 | 58.6 |
| 3.30 | 88.5 |
| 3.25 | 123.4 |
| 3.19 | 161.5 |
| 3.14 | 205 |
| 3.09 | 270 |

**Table 4** Conductivity data for [ImPr][Phth] by temperature

| **1000/T ($K^{-1}$)** | **conductivity (μS/cm)** |
|---|---|
| 3.28 | 37.8 |
| 3.28 | 38.3 |
| 3.28 | 39 |
| 3.28 | 41.9 |
| 3.28 | 41 |
| 3.28 | 40 |
| 3.28 | 43.2 |
| 3.28 | 44 |
| 3.28 | 47.2 |
| 3.27 | 48.7 |
| 3.27 | 50.8 |
| 3.27 | 51.5 |
| 3.26 | 52.6 |
| 3.26 | 54 |
| 3.26 | 55.1 |

| | |
|---|---|
| 3.26 | 56.7 |
| 3.26 | 58 |
| 3.25 | 59.4 |
| 3.25 | 61 |
| 3.24 | 75.3 |
| 3.23 | 77 |
| 3.23 | 80 |
| 3.23 | 86 |
| 3.22 | 92 |
| 3.21 | 96.7 |
| 3.21 | 101 |
| 3.20 | 110 |
| 3.20 | 114 |
| 3.20 | 118 |
| 3.19 | 122 |
| 3.19 | 127 |
| 3.19 | 132 |
| 3.18 | 141 |
| 3.17 | 170 |
| 3.17 | 175 |
| 3.17 | 183 |
| 3.16 | 189 |
| 3.16 | 200 |
| 3.16 | 210 |
| 3.15 | 222 |
| 3.15 | 233 |
| 3.13 | 260 |
| 3.12 | 282 |
| 3.11 | 310 |
| 3.11 | 330 |
| 3.10 | 360 |
| 3.09 | 384 |
| 3.08 | 416 |
| 3.08 | 442 |

| | |
|---|---|
| 3.08 | 470 |
| 3.07 | 508 |
| 3.06 | 537 |
| 3.04 | 587 |
| 3.04 | 625 |
| 3.02 | 702 |
| 3.02 | 708 |
| 3.02 | 704 |
| 3.01 | 740 |
| 3.01 | 790 |
| 2.98 | 860 |
| 2.98 | 924 |
| 2.96 | 1000 |
| 2.94 | 1063 |
| 2.94 | 1111 |
| 2.91 | 1133 |
| 2.90 | 1260 |
| 2.87 | 1440 |
| 2.82 | 1770 |
| 2.81 | 1860 |
| 2.79 | 1940 |
| 2.78 | 2030 |
| 2.76 | 2100 |
| 2.74 | 2200 |
| 2.73 | 2300 |
| 2.73 | 2410 |
| 2.69 | 2610 |

## V. Crystalline structure

The crystalline features of [ImPr][Ox] and [ImPr][Phth] were assessed by scanning electron microscopy (SEM). A JEOL JSM-5600 SEM operating at 15 kV was used to obtain the images.

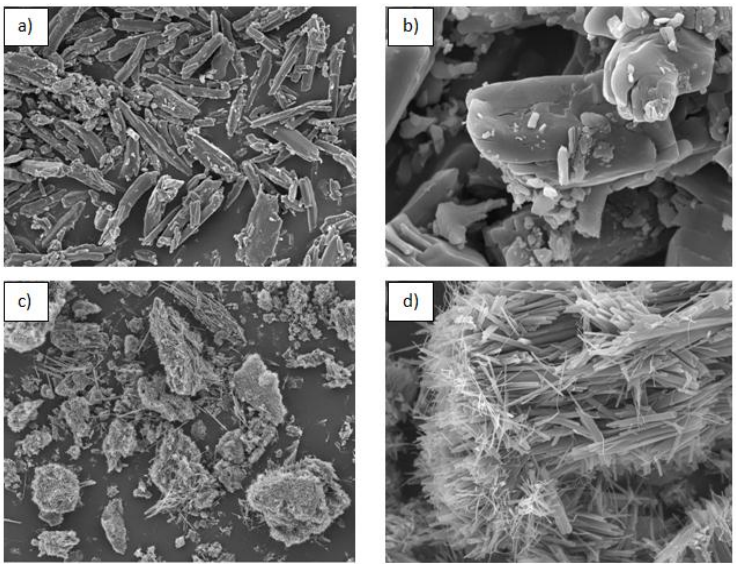


**Figure S10** a) SEM image of [ImPr][Phth] at 100µm zooming b) SEM image of [ImPr][Phth] 10 µm zooming c) SEM image of [ImPr][Ox] at 100µm d) SEM image of [ImPr][Ox] at 10 µm zooming

SEM images were obtained of the surface of solid samples prepared by melting the powder and subsequent solidification, the samples were then coated with a 10 nm layer of gold to ensure good surface conductivity. SEM micrographs of the surface of [ImPr][Phth], [ImPr][Ox] and [ImPr][$HSO_4$] were recorded and shows in Figure S12.

The crystalline features have been observed for all these three samples. Due to the high sensitivity of the [ImPr][$HSO_4$] to the beam, the image did not have a good quality. Both [ImPr][Ox] and [ImPr][Phth] samples show needle-shaped morphology.

## VI. Density measurement

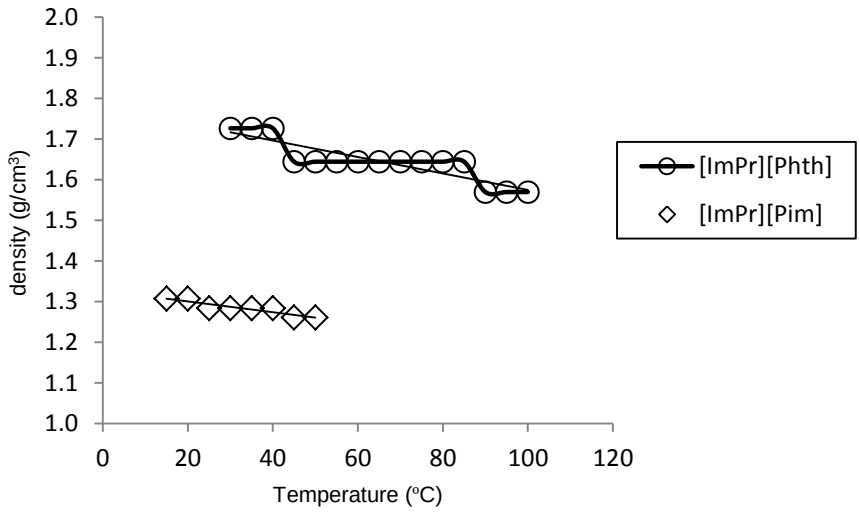


**Figure S11.** Changes in densities by temperature for selected PILs in this study

## VII. Crystal structure

Detail of the xray crystallography experiments is available in CIF file.

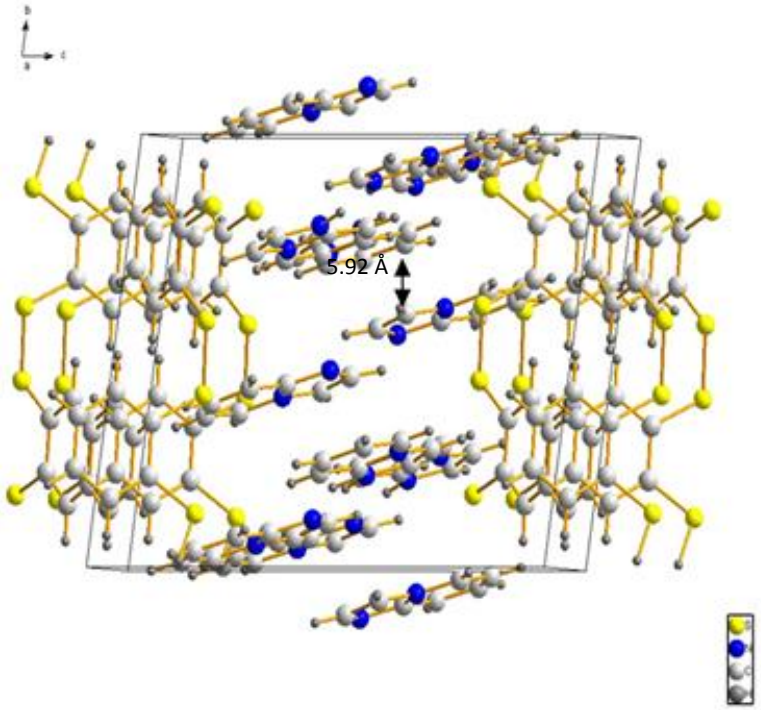


**Figure S12.** Ion packing in the crystal structure of [ImPr][BDT]. The distances of the aromatic rings between ionic and molecular ImPr are 5.92 Å. Viewed along the a-axis

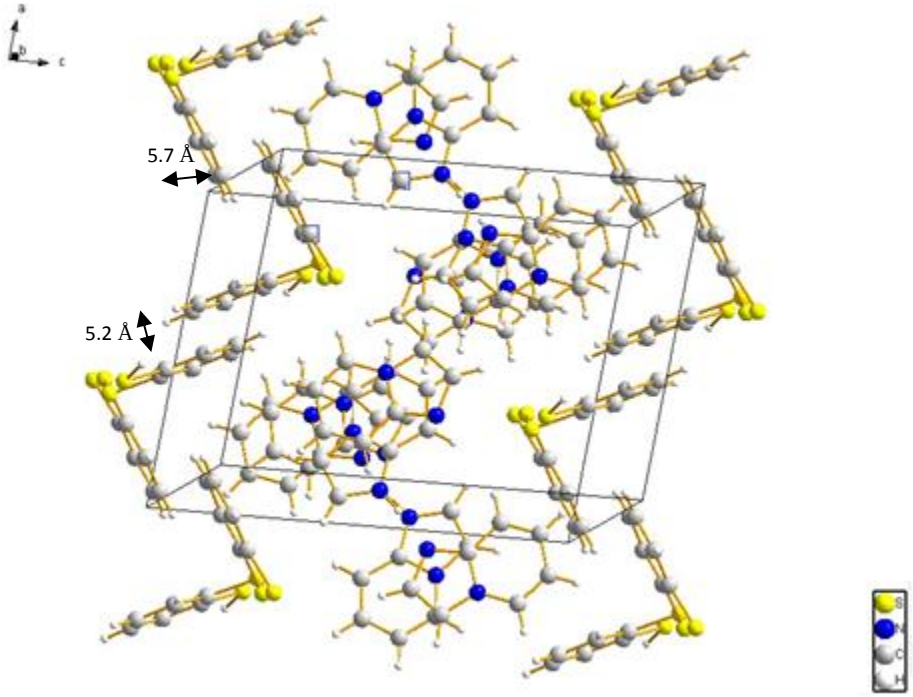


**Figure S13.** Ion packing in the crystal structure of [ImPr][BDT]. The distances between the aromatic rings of benzene-1,2- thiolate/disulfide are 5.2-5.7 Å. Viewed down the b-axis